



Degree Project in Aeronautical Engineering

First cycle, 15 credits

Electrical Propulsion System Design of a Blended Wing Body UAV

Project Green Raven

Kevin Azad
Felix Fungula

Authors

Kevin Azad <kazad@kth.se>
Felix Fungula <ffungula@kth.se>
Aeronautical Engineering
KTH Royal Institute of Technology

KTH Royal Institute of Technology

Stockholm, Sweden

Examiner

Per Wennhage
Gunnar Tibert
KTH Royal Institute of Technology

Supervisor

Raffaello Mariani
KTH Royal Institute of Technology

Abstract

The conventional tube-and-wing aircraft has been around since the 1950s, with little to no innovative progress being made towards redesigning the conventional aircraft. The blended wing body (BWB) shape fuses the wing of the aircraft with the fuselage increasing structural strength while also increasing potential surface area to create lift, making it more efficient than conventional wing shapes. Today aviation has a 2 % CO_2 contribution to global emissions. Aircraft manufacturers are predicting a steady rise for the aviation industry. The contribution of greenhouse gases is set to increase exponentially. Hydrogen fuel cells could deem a good fit between traditional combustion engine aircraft and electrical aircraft having a high efficiency but also being fuel-based. This report investigates the possibility of a prototype model of the Project "Green Raven" from KTH of creating a hybrid fuel cell BWB UAV with a 4 m wingspan. The analytical data is from literature and available benchmark data. First, an electrically driven subscale prototype is made and tested, and then the full-scale model is made. The prototype is proposed to be driven by a single two-bladed propeller with 10 x 4.7-inch dimensions running at 10000-13000 rpm with a takeoff weight of 4 kg, where 0.75 kg of the weight was from 5 Li-Po batteries. Performance parameters were calculated by given data with a given cruise speed of 30 m/s and a cruise endurance of 1 hour. The prototype will fly for close to maximum load at climb with an angle of 6° . With the Li-Po batteries with a total of 11 Ah, the aircraft has more than 10 % to spare for safety reasons.

Sammanfattning

Den konventionella tub och ving flygplanet har funnits sedan 1950-talet med få innovativa framsteg gjorda för att revolutionera det konventionella flygplanet. Den hybrida ving kroppen smälter samman vingen med kroppen av flygplanet vilket gör strukturen starkare och ökar ytan som kan skapa lyft vilket gör planet mer effektivt än konventionella vingformer. Idag så står flygindustrin för ca 2 % av globala utsläppen av CO_2 . Flygplanstillverkare förutser att flygandet kommer fortsätta öka för flygindustrin. Utläppet av växthusgaserna kommer då stiga exponentiellt. Vätebränsleceller skulle kunna fylla en plats mellan den konventionella förbränningsmotorn och elektriskt drivna flygplan då de har en hög effektivitet men fortfarande är bränsledrivna. Den här rapporten undersöker en prototyp av en modell av "Green Raven" Projektet från KTH som bygger en hybrid bränsle-cells driven hybrid ving kropp UAV med en vingbredd på 4 m. Analysen baseras på litteratur och test referensdata. Först byggs en mindre elektriskt driven prototyp som testas och sedan byggs den större modellen. Prototypen föreslås att drivas av en enmotorig propeller med 10 x 4.7 tum dimensioner med 2 blad som drivs runt 10000-13000 rpm med en flygvikt av 4 kg där 0.75 kg bestod av 5 Li-Po batterier. Parametrar för prestanda beräknades av given data med marschfart på 30 m/s och en uthållighet vid marsch på 1 timme. Prototypen kommer flyga nära max effekt vid stigning med en stigvinkel på 6°. Driven av Li-Po batterier med totalt 11 Ah kommer flygplanet ha mer än 10 % extra energi för säkerhet.

Acknowledgements

We would like to thank our supervisor Raffaello Mariani for his guidance and support throughout the project. We would also like to thank KTH for giving us access to information, books and articles which has been crucial for the research.

Nomenclature

a	Acceleration
b	Wingspan
c	Chord
C_D	Drag coefficient
C_L	Lift coefficient
C_P	Power coefficient
C_T	Thrust coefficient
D	Drag
E	Endurance
g	Acceleration due to gravity
I	Current
J	Advance ratio
L	Lift
m	Mass
P	Power
R	Range
S	Wing area
T	Thrust
t	Time
U	Voltage
V	Speed
W	Weight
α	Angle of attack
η	Efficiency
μ	Atmospheric viscosity
ρ	Atmospheric density

Acronyms

AOA Angle of Attack.

AOC Angle of Climb.

AOD Angle of Descent.

AR Aspect Ratio.

BWB Blended Wing Body.

CG Centre of Gravity.

DOC Depth of Discharge.

FOV Field of View.

ROC Rate of Climb.

ROD Rate of Descent.

SOC State of Charge.

UAV Unmanned Aerial Vehicle.

Contents

1	Introduction	1
1.1	Background	1
1.2	Sustainable Aviation	1
1.3	Blended Wing Body	2
1.4	Project "Green Raven"	2
1.5	Purpose	3
1.6	Requirements	4
1.7	Objectives and Mission Profile	5
1.8	Limitations	5
2	Theory and Methodology	6
2.1	Performance	6
2.1.1	Takeoff	7
2.1.2	Climb	8
2.1.3	Cruise	9
2.1.4	Descent	9
2.1.5	Landing	10
2.2	Range and Endurance	10
2.3	Propeller	11
2.3.1	Propeller Design	13
2.4	Battery	13
2.4.1	Battery degradation	14
2.5	Drivetrain	15
2.5.1	Motor trade study	15
2.5.2	Battery Trade Study	16
3	Results	17
3.1	Total Weight and Cost	17
3.2	Propulsion	17

3.3	Battery	20
3.4	Three-segment mission	21
3.5	Mechanical Design and Integration	24
4	Discussion	25
5	Conclusion	27
6	Future Work	27
	References	29
A	Appendix	i
A.1	Aerodynamic Properties	i
A.2	Benchmark of Motordata	iii
A.3	CFD Data	v

1 Introduction

1.1 Background

In the future to come, demands on air and space travel is constantly evolving. With emissions rising, new demands on the efficiency of aircraft are made. The conventional tube-and-wing aircraft has been in use for more than half a decade with little to no innovative progress toward redesigning the conventional aircraft. Today's conventional planes are based on the same engine and overall design implemented by the Boeing 707. New innovative technology leaps need to be made.

1.2 Sustainable Aviation

The problem with aviation is the amount of environmental footprint it will have on the environment. Today the aviation industry accounts for around 2 % CO_2 contribution to global emissions, with its total emissions set to rise in the coming years. With a majority of the world population never have set their foot in a plane, and with flight set to become accessible to a greater part of the population. Aircraft manufacturers are predicting a steady rise in aviation and flights [1]. The contribution of greenhouse gases is set to increase exponentially. The aviation industry is a case in point of the Jevons paradox. The effectiveness of the motors and lift to drag ratio have steadily increased. With the emissions per flight mile decreased but the total output overall emission has however increased due to increase in flying, which increases with about 5 % on a yearly basis. In order to reduce the effect on the environment, different actions have to be taken. Conventional aircraft can only reduce emissions by making aircraft more efficient using lightweight materials and new engine innovations [2].

With electrical aircraft the dependence on carbon-based fossil fuel is diminished and the output of carbon and NO_x emissions goes down. Apart from this a fully electrical aircraft can in theory have higher efficiency, greater reliability, less maintenance and less noise than conventional combustion engines. With an increase in electrical technology the cost of flying an aircraft can reduce since the highest operating cost of an aircraft is fuel. The problem is the amount of weight technology such as batteries add to the aircraft which still needs development [3].

Hydrogen fuel cells have an efficiency between 41-49 % whereas electrical vehicles have a higher efficiency, hydrogen fuel cells can be refueled in 10 minutes which is an advantage compared to batteries. They also do not need the weight of batteries which is the bulk of weight in an electric vehicle (apart from chassis) [4].

1.3 Blended Wing Body

The first experiments and patents of a "*Flying Wing*" were made around 1910. The development was primarily made in Germany. In 1950 the Northrop Corporation developed and tested the N-1M. The plane flew, but the stability was a major showstopper as flight-by-wire technology was not fully developed yet. Today technology has evolved, and the US military's B-2 is a current example of a successful implementation of the flying wing [5].

The blended wing body (BWB) is an offshoot of the flying wing. With the fuselage and wings blended together in a continuous form, a BWB fuses the wing of an aircraft with its fuselage, creating a bigger surface that can be used to create lift with increasing efficiency. This gives it a few advantages over conventional tube-and wing aircraft. Since the body, fuselage, and tail are one component, it is more effective, meaning in practical terms that the aircraft can be made smaller and cheaper. The blended wing body allows for a more extensive area in which lift is created while also having higher structural efficiency. As the lift is divided more equally, the load is closer to the ideal load curve. This dramatically reduces the bending stress on the wings compared to a conventional tube-and wing plane. This enables weight reduction. The more equally distributed lift also induces fewer vortices which contributes to less drag. The fuselage and the tail on a conventional aircraft induce a lot of drag and have no function other than storing payloads such as humans or cargo while also reducing noise since the placement of the engine can be placed so that the sound waves are reflected upwards. Given this, a BWB aircraft can be made with up to 20 - 25 % - less power consumption [2].

The drawbacks of a BWB compared to a conventional aircraft includes the difficulty of cabin pressurization of a non-round fuselage and the stabilizing function of the tail. It also lacks a horizontal tail stabilizer. Given this, it is indispensable for a safe flight that a flight computer handling the flight surfaces is required to keep the plane stable. Even then, a BWB typically stalls at a lower angle of attack and has less ability to recover from a stall.

1.4 Project "Green Raven"

Project "Green Raven" is a KTH-driven project where sustainability and the world of unmanned aeronautics are met. The project consists of a hybrid/electrical driven BWB UAV using hydrogen fuel cells with batteries which leads to a low ecological footprint as well as good performance. The dimensions are set with a wing span of 4 m and a maximum allowed takeoff mass of 25 kg for the full scale aircraft.

This project focuses on designing the propulsion system for a small scale prototype of this model for future testing and as a gateway into the full scale Project "Green Raven" aircraft. Dimension will be 1.5 m and maximum allowed takeoff mass of 7 kg. The UAV

will use a propeller as its means of propulsion. A CAD rendered image of the small prototype is shown in figure 1.

The UAV as an alternative to manned aircraft, because of the fact that no human is onboard the aircraft it can be used for more dangerous missions and surveillance missions that take a long amount of time. They are in general smaller and either remote controlled or controlled using autonomous navigation [6].

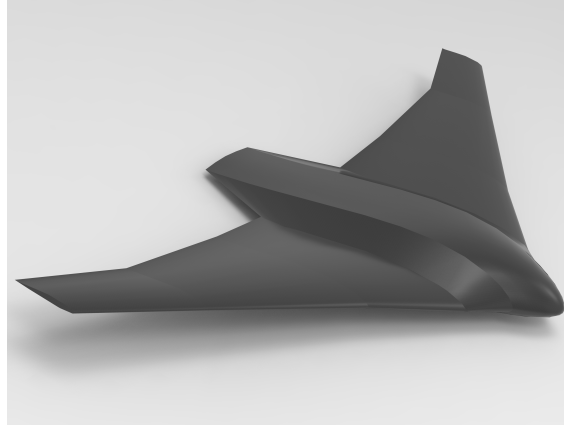


Figure 1: Rendered CAD image of the subscale Project "Green Raven" Prototype from KTH

1.5 Purpose

The mission largely follows how a prototype for a new aircraft typically is made and especially the work made in a collaboration between McDonnell Douglas/Boeing and NASA during the 1990s when they made the first efforts for a BWB [5].

First, a "mule" aircraft will be developed. The mule will be a simple aircraft flight controls to have similar flight characteristics as a BWB. This is to ensure that the in-house capabilities exist and to train on remotely flying a plane with the flight characteristics of a BWB. Then a 30 % scaled version of the Project "Green Raven" will be built, which the power system in this report is designed for. The primary purpose of this scaled version is to evaluate the flight characteristics and the aerodynamics.

The thrust to weight ratio is aimed to be close to that of the full-scale plane. Just as in the full-scale version, lightweight material will be used. The propulsion will be electric with propellers. This is to get as close to the aim of an electric/hydrogen hybrid system as possible. In the last step, the full version will be built with the full wingspan of 4 m and a hybrid system of hydrogen and electric propulsion.

1.6 Requirements

The aircraft will need to be modeled using two configurations. Launched using a rail launcher where it will belly land on soft grass and in the other configuration using conventional non-retractable tricycle tires where it launches as a conventional aircraft on a runway without brakes. The aircraft will need to complete a mission flying from point A to point B and back with enough power for the flight with about 10 % in reserve for safety reasons. It will have 1 hour in cruise flight time where the range of the flight will be calculated.

- Cruise a duration of 1 hour at a constant velocity of 30 m/s
- It's maximum takeoff weight is allowed to be 7 kg
- Material will be out of EPP foam
- It will have solid wings
- It will have shell-like fuselage of 5 mm thickness
- It will be propeller driven
- It will have no flaps instead use control systems
- It will takeoff by launcher with rails or tricycle tires using a runway

Here is the given data for the aircraft:

Table 1: Given Data

Parameter	Meaning	Value (unit)
m	Aircraft shell weight	3 [kg]
S	Wing area	0.405 [m ²]
c	Chord	0.36 [m]
b	Wing span	1.5 [m]
AR	Aspect ratio	5.55 [-]
ρ	Atmospheric density	1.225 [kg/m ³]
μ	Atmospheric viscosity	$1.74 \cdot 10^{-5}$ [Ns/m ²]
V_{cruise}	Cruise velocity	30 [m/s]
t_{cruise}	Cruise time	3600 [s]
g	Acceleration due to gravity	9.82 [m/s ²]
$C_{L_{max}}$	Maximum lift coefficient	0.789 [-]

1.7 Objectives and Mission Profile

- Choose propeller dimensions based on calculations/benchmark data
- Calculate performance (takeoff, climb, cruise, range, endurance and descent) while keeping BWB flight characteristics
- Choose appropriate motor configuration based on calculations/benchmark data
- Choose batteries based on Endurance, Range and motor chosen

The mission profile of the aircraft will *takeoff* using a rail launcher and/or a runway and will then *climb* to the desired altitude of 100 m at which it will then commence its *cruise* phase which it will fly for 1 hour, with spare energy the aircraft then *descends* 100 m with the motor at 10-20 % power and belly land on soft grass without tires or land on dry asphalt with tires which will be the final phase of *landing*.

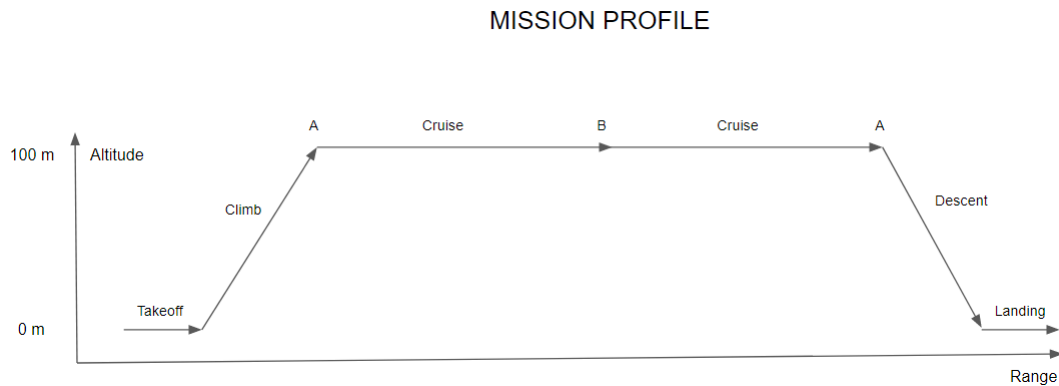


Figure 2: Mission Profile for a standard mission from point A to B and back.

1.8 Limitations

- The propeller size if more than one is limited by the space and construction of the drone since it will be launched using a rail launcher and the limited tail space
- The dimensions of the aircraft are fixed and cannot be altered
- Swedish laws affect weight above 7 kg making it more troublesome for flying UAV by demanding permits
- Stalls are more dangerous since it will fly over residential area
- The project requires a propeller so ducted fans and other types of propulsion will not be covered

2 Theory and Methodology

2.1 Performance

Performance is a description of how a plane moves and the energy and power it takes to perform those maneuvers. A wide range of factors have to be taken into consideration. The performance is usually divided into different flight maneuvers. The maneuvers that will be analyzed are:

- Takeoff
- Climb
- Cruise
- Turns
- Descent
- Landing

All calculations in the *Theory and Methodology* take no consideration to wind and are all taken from Gudmundsson [7].

Lift is the aerodynamic force produced by the wings, and in this case, by the body and the reason planes can stay in the air. It has the following formula:

$$L = \frac{1}{2}\rho V^2 SC_L. \quad (1)$$

Drag is the force counteracting the movement of the plane taking into account both skin friction and form drag:

$$D = \frac{1}{2}\rho V^2 SC_D. \quad (2)$$

An important relationship is lift-to-drag ratio:

$$\frac{L}{D} = \frac{C_L}{C_D}. \quad (3)$$

Central for the whole performance part is the stall speed. The stall speed is a threshold at which there is a high risk that the plane will not be able to generate enough lift to stay

in the air. The lift is proportional to the speed and given this a minimum stall speed is often used. Stall usually occurs suddenly and can be hard to recover from. The stalling speed is given by:

$$V_{stall} = \sqrt{\frac{2W}{\rho S C_{L,max}}}. \quad (4)$$

2.1.1 Takeoff

Takeoff is a decisive part of the flight because of the sensitivity of the flying and the possibility of stalling at takeoff, which occurs when the aircraft cannot create enough lift to counteract the weight. During takeoff, it is crucial to have enough lift to keep climbing to a safe altitude at which a plane can start flying at a cruising speed [6].

For a rail launcher or bungee cord, the speed at the end of the launcher needs to be $V_L \approx 1.2V_{stall}$, that gives the velocity needed to start flying as soon as the aircraft leaves the launcher [8]. If the propulsion system is turned off during the launch, a higher velocity has to be achieved to account for the time it takes for the system to start generating thrust.

The two most common configurations for a conventional takeoff with a landing gear are taildragger and tricycle. Since the plane in question has virtually no tail, the most appropriate set-up would be tricycles. The tricycle has 3 contact points with the runway, with 2 in the back and one in the front shown in figure 3.

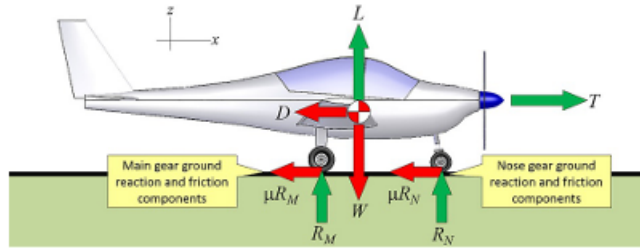


Figure 3: Free body diagram of takeoff with landing gear from [7].

The landing gear usually adds at least 5 % to the weight of the plane, and the addition to the parasitic drag of the landing gear can be as high as 15 - 28 % [9]. It can however be significantly reduced using techniques such for example the applications of fairings [10]. The extra drag from the landing gear will not be accounted for.

The speed which the plane needs to takeoff is generally $V_{takeoff} = 1.1V_{stall}$.

The distance needed for takeoff is determined by the speed and acceleration of the aircraft. Lift, drag and their respective coefficients is affected by the velocity. Furthermore, Lift and drag effect the acceleration. This makes the need for a integration scheme where each repetitive value is used for that time and speed interval where it is relevant. Each time interval is then added up to make the total distance.

Ground effect is an important part of takeoff since it affects the AOA and lift required because of forces caused by the aircraft being close to the ground, this reduces drag and increases lift slightly making the AOA needed to be lower to gain the same amount of lift, potentially making the AR more efficient. The ground effect is especially prominent on BWB configurations.

The actual effect the ground has on an aircraft is:

$$\Delta a_i = -\frac{C_L}{\pi \cdot AR} e^{-2.48(2h/b)^{0.768}}. \quad (5)$$

2.1.2 Climb

Climb is the part of the flight after the aircraft has left the ground and is gaining altitude in order to have a safe altitude to then fly at a cruising speed. Obstacle avoidance is of primary importance during the climb, especially just after takeoff. Therefore, the minimum safe climb gradient is a predominant requirement during the takeoff climb. To gain altitude as fast as possible, it is necessary to fly at maximum ROC [7] [11].

For a conventional aircraft stall typically occurs around a 15° AOA. For a BWB the stall has been shown to appear at a lower AOA. The climb angle should be below the stall angle with a good safety margin around where C_L/C_D is the lowest for maximum efficiency. Finding the ROC and distance flown during climb is essential. The climb speed generally has to be $V_{climb} \geq 1.2V_{stall}$.

The amount of thrust needed to hold a certain angle is:

$$T = D + (W \cdot \sin\alpha). \quad (6)$$

The power required during climb (assuming climb angel $\cos\alpha \approx 1$) is:

$$P = DV. \quad (7)$$

In order to calculate ROC and Range the respective components of the velocity needs to be calculated:

$$V_V = V_\infty \sin \gamma, V_H = V_\infty \cos \gamma. \quad (8)$$

Where V_V is the ROC and V_H can be used to calculate distance flown during climb.

2.1.3 Cruise

Cruise is the part where the aircraft will fly most of the duration. When flying at cruising speed, it is essential to fly at maximum C_L/C_D in order to use as little energy as is possible in order to maximize distance flown. During cruise, descent will be 0 i.e $L = D$ and $D = T$. *Steady-level turns* meaning turns that are absent of acceleration or a change in altitude. If thrust available exceeds thrust required, the aircraft will accelerate.

The power required for level flight for a particular angle α is:

$$P = \sqrt{\frac{2W^3 C_D^2}{\rho S C_L^3}}. \quad (9)$$

The stall speed while in a turn with angle ϕ will be:

$$V_{stallturn} = \frac{V_{stall}}{\sqrt{\cos \phi}}. \quad (10)$$

To maintain altitude and airspeed when executing a turn both the AOA and the thrust have to be increased above their level flight values.

This gives the turn radius:

$$r = \frac{V_{stallturn}^2}{g \cdot \tan(\phi)}. \quad (11)$$

The time to turn ψ degrees:

$$t = \frac{r}{V} \left(\psi \frac{\pi}{180} \right). \quad (12)$$

2.1.4 Descent

Descent is the part when the aircraft is losing altitude, and it is crucial to have enough power to fly back to the landing area or in case of an emergency. Performing a powered

descent is safer because the motor has power in case something occurs, as well as allowing for better control. Unpowered descent is more environmental as you can use the aircraft as a glider and not consume any energy. Flying at a high L/D can become a problem during landing since the AOA is not as steep, making it harder to pinpoint where you touchdown. Having the motor running at 10 - 20 % allows for a further range while not using too much energy.

The velocity needed for this to hold the angle α is:

$$V_{descent} = \sqrt{\frac{2\cos\alpha}{\rho C_L} \left(\frac{W}{S}\right)}. \quad (13)$$

Since angle-of-attack is now inverted the velocities which gives ROD are:

$$V_V = V \sin\alpha, V_H = V \cos\alpha. \quad (14)$$

2.1.5 Landing

Before landing, when approaching the runway, a decrease in the vertical speed at which touchdown occurs during landing has to be made. An unpowered landing without landing gear will be done by a "belly landing" with engines turned off at touchdown and with landing gear without brakes that also have the engines turned off at touchdown. Where the touchdown speed is $V_{touchdown} = 1.1V_{stall}$. The landing distance can be calculated with equation ?? using $V = V_{touchdown}$.

The deceleration needed to stop is:

$$a = \frac{g}{W} [T - D - \mu(W - L)]. \quad (15)$$

2.2 Range and Endurance

Range and Endurance are performance parameters explaining the time an aircraft can stay in the air, *Endurance*, and the amount of distance an aircraft can fly, *Range*. For an electrical aircraft, weight does not change during the flight since fuel is not being used.

Time in hours to drain the battery which in this case is the endurance becomes:

$$\Delta t = \frac{E_{Batt}}{P_{Batt}}. \quad (16)$$

The actual amount of available motor power we have is:

$$P_{AV} = \eta_{tot}P. \quad (17)$$

Since this is an electrical aircraft, power degradation and efficiency are of concern. The no wind Range is given by:

$$R = V_{\infty}\Delta t = V_{\infty} \frac{E_{batt}}{P_{batt}} = V_{\infty} \frac{\eta_{tot}E_{batt}}{P_{AV}} = \frac{\eta_{tot}E_{batt}}{W} \left(\frac{C_L}{C_D} \right). \quad (18)$$

Equation 18 can be simplified into eq. 19 to give the Endurance:

$$E = \frac{\eta_{tot}E_{batt}}{WV_{\infty}} \left(\frac{C_L}{C_D} \right). \quad (19)$$

2.3 Propeller

A propeller creates thrust and an aircraft uses that thrust to create lift, it does that by the same principle of wings. The propeller consists of multiple blades set at an angle, in this case a fixed-pitch propeller.

The efficiency η will determine how much of that power from the propeller goes into making usable thrust. It depends on the angle of attack, rpm and airspeed. Since the focus of this aircraft is the *cruise* part of the performance, a fixed-pitch "cruise" propeller should be the focus. A propeller with higher efficiency at a higher speed and climb is not as relevant. The propeller formulas were used from Gudmundsson [7].

The power and thrust coefficients are given by:

Power coefficient:

$$C_P = \frac{P}{\rho n^3 D_p^5}. \quad (20)$$

where P is the power of the motor, n being the rpm and D_p being the propeller diameter.

Thrust coefficient:

$$C_T = \frac{T}{\rho n^2 D_p^4}. \quad (21)$$

The steps for deciding on a propeller are as follows:

1. Calculate propeller diameter D_p for 2 blade propeller regardless of material:

$$D_p = 0.56 \sqrt[4]{0.001 \cdot P}. \quad (22)$$

2. Estimation of propeller pitch at cruising speed:

$$P_G \approx 2432 \frac{V}{RPM}. \quad (23)$$

3. Determine advanced ratio:

$$J = \frac{V_\infty}{nD_P} = \frac{60 \cdot V_\infty}{RPM \cdot D_P}. \quad (24)$$

4. Estimation of required propeller efficiency:

$$\eta_p = \frac{TV_\infty}{P} = J \frac{C_T}{C_P} = \left(\frac{T}{W} \right) \frac{W \cdot V}{P} = \frac{WV_\infty}{(L/D)P}. \quad (25)$$

The number of blades a propeller has also matters, the most common are 2 bladed propellers. As airspeed increases, so does efficiency until a certain speed. Efficiency is highest with 2 blades at a low airspeed, but thrust and power increases as blade number increases. Figure 4 shows how blade count compares depending on velocity.

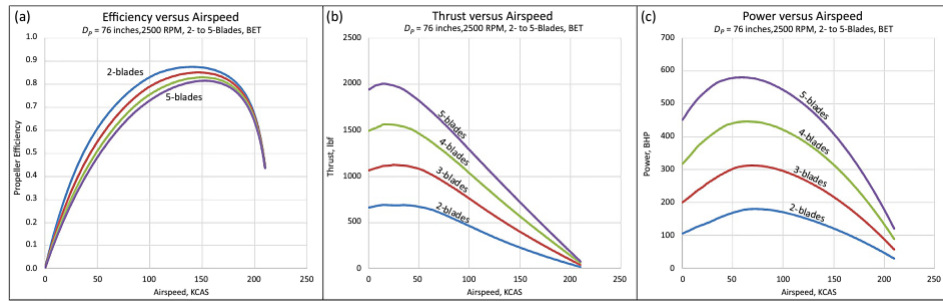


FIGURE 15-32 Effect of number of blades on a propeller's efficiency, thrust, and power.

Figure 4: Propeller efficiency of multiple blade configurations. Efficiency vs airspeed to the left, thrust vs airspeed in the middle and power vs airspeed to the right [7].

The most common type of propeller configurations are *Tractor*, *Pusher* and *Nacelle* configurations.

With the Tractor configuration, the propeller is in front of the plane by the engine. This gives the propeller more clean air and is less affected by the wing causing disturbance

on the air. With the Pusher configuration, the propeller is behind the fuselage of the plane. This will suppress flow separation on the body but, at the same time, may cause difficulty at landing since the propeller is closer to the ground. With the Nacelle configuration, multiple propellers are mounted similar to the Tractor configuration but are more efficient. Because the propellers are mounted further out on the wings, higher structural load is induced [7].

2.3.1 Propeller Design

In order to calculate performance parameters some values must be chosen in advance based on given data in appendix A.1 and A.3. Different propeller sizes were calculated based on power usage and in a dual and single propeller configuration. Trade studies were made to compare different batteries and their respective capacitance.

For the launcher the motor will be turned off or at idle since it can be damaged while being launched. Data from the launcher is taken from Sadraey [8].

When modelling the propeller, the aim is to optimize the size and efficiency for the requirements. The data received regarding lift and drag shows at what angle this prototype will be flying at for maximum efficiency. Modelling for a dual and single propeller configuration will be done to compare and contrast since a dual propeller setup can be used as a part of the flight control if each engine runs at different rpm, a two versus three bladed configuration in each regard will also be made. The motor will run at about 80 % of full power during cruise in order to prevent overheating of the motor.

2.4 Battery

The energy drawn from the battery is divided into two parts. The power drawn by the motor and power train and the power drawn by the system, including lights, avionics, communication, and the fly by wire system. This study will only focus on the energy drawn by the drive train.

A battery can be connected in parallel to get more capacity or in series to get a higher voltage. How much voltage is needed is mostly dependent on the motors and the rpm wanted. C-rating is a rating that is given with most batteries and it gives the maximum AMP the battery can handle. It is usually a continuous C-rating and a burst rating that is only applicable for a short time. What C-rating that is needed is based on the I_{max} that is required by the motor.

The I_{max} that the motor can handle can be calculated with:

$$I_{max} = C_{rating} \cdot C. \quad (26)$$

Internal resistance is another important factor to calculate when using batteries as power. It is mostly not given and it varies with age and usage of the battery. It can however be measured. The battery efficiency of Li-Po is above 95 % [12].

2.4.1 Battery degradation

Battery degradation is usually divided into cycling and aging. Cycling being the depletion of charge and aging being the effect of age. The causes of degradation are many, the most prominent causes are solid electrolyte interphase (SEI) layer growth, particle fracture and lithium plating. Adding all these can have a degradation effect on the energy capacity of up to 60 % over 100 cycles in extreme cases. Making it an important consideration when choosing battery capacity [13].

One of the main catalyst of battery degradation is high temperatures, as any temperature above 25° is adding to degradation. This effect is most prominent during cycling. As it isn't an implementation of cooling on the aircraft it is a risk of temperatures above 25°C. Adding to the degradation will be that the SOC will be from a 100 % to 10 - 20 %, which is not ideal as going to a low SOC add to the degradation effect. To keep the aging at a minimum a SOC should not be over 50 %. The aging part will most likely to have a minimal effect as the aircraft will have its location in Sweden where the climate is seldom above 25°C.

Based on other studies and given the factors stated above a battery safety margin of 15 % will be added to the battery capacity requirement. It is recommended that the batteries should also be placed in a way so that they are easily replaced [14]. As with all aircraft, an additional battery reserve has to be kept in case the flight route has to be changed or an emergency occurs. For this purpose another 10 % battery capacity has been added to the calculations of the total amount of capacity for the battery.

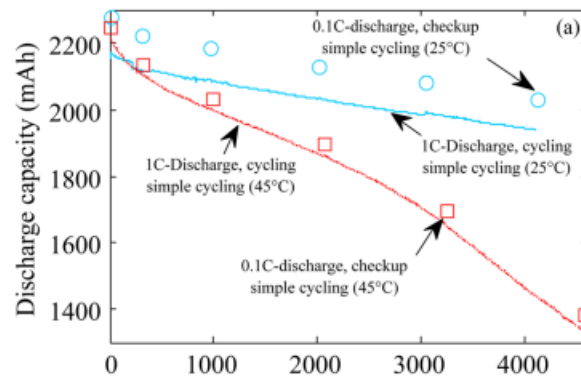


Figure 5: Battery Degradation of a Li-Po battery over cycling. Degradation in 25 °C (Blue line) and in 45 °C (Red line) ambient temperature. From the article [14].

2.5 Drivetrain

In order to get sufficient amount of energy running to the motors different batteries were compared with regard to the efficiency, size and weight.

2.5.1 Motor trade study

Brushed and brushless Motors: The study is focused on brushless motor given their superior efficiency, less maintenance, longer life expectancy and low noise. They are however more expensive. An other factor narrowing down the choice of motor is an outrunner because of the increased torque over inrunners.

In the first stage of the trade study three motors manufacturer were compared: Emax, Leopard and SunnySky. The study then further studied the different models of the Leopard LC2835. Benchmark data in appendix A.2 were used to predict the real power output of the motor. From the calculated propeller diameter and pitch the motors were compare though benchmark data. An exact benchmark with the calculated propeller dimension could not be obtained. The focus was to find benchmark data with comparable propeller configurations.

- Cost
- Efficiency
- Weight
- Thrust output

- Size
- g/W

2.5.2 Battery Trade Study

A wide range of batteries were investigated with a main focus on lithium-polymer batteries given their energy density and power output. The batteries main purpose is to supply the motor with enough power. Given the Leopard motor which has a recommended use with a 2-3S battery, meaning that 3 batteries is series giving a 11.1 V nominal voltage, was going to be used. The minimum capacity need to fulfill all the mission requirements including safety margin. All the batteries in the study are from the brand GensAce. The trade study was based on the following conditions:

- Cost
- Power density
- Total weight
- Power output
- Size
- Max Amps

3 Results

3.1 Total Weight and Cost

The weight of the aircraft was kept to a minimum as a high weight will reduce the thrust and power required while also not needing more since the additional control systems and instruments won't increase the weight drastically. The weight is given by the aircraft itself as well as 1 motor, 1 propeller and 5 batteries added total.

Table 2: Weight and Cost per component.

Object	Weight	Cost
Body	3 kg	[-]
Mounting	0.25 kg	[-]
Propeller	≈ 0 kg	50 kr
Motors	0.1 kg	260 kr
Batteries	0.75 kg	800 kr
Total	4 kg	1110 kr

3.2 Propulsion

In figure 6 where the lift to drag ratio reaches it peak at 2° is where the cruising angle will be for optimal range.

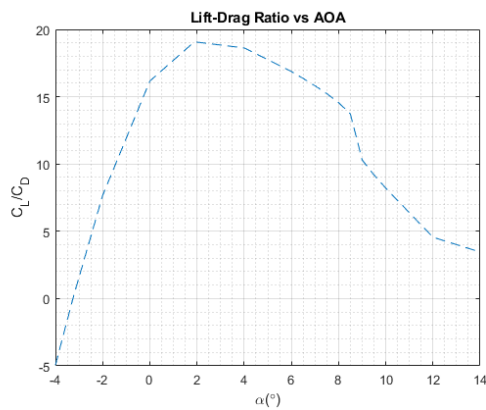


Figure 6: Lift-Drag Ratio vs AOA

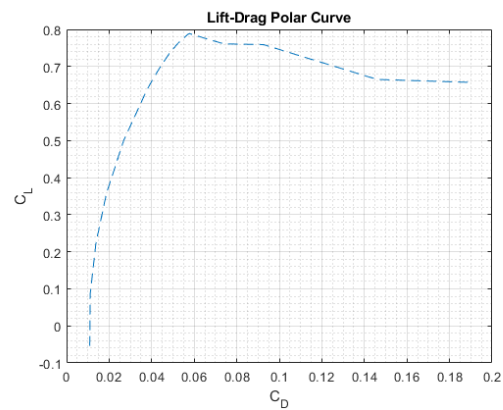


Figure 7: Lift-Drag Polar Curve

Where it shows the stall angle at 8° .

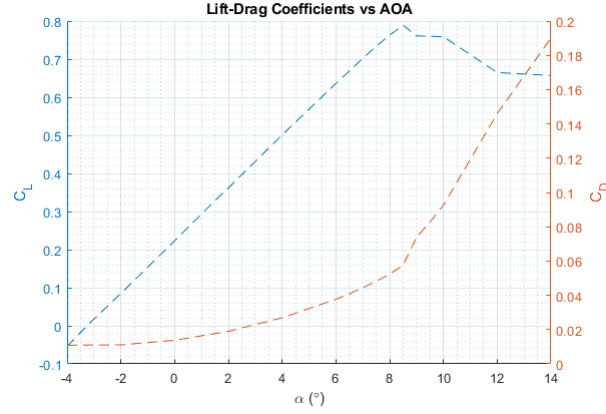


Figure 8: Lift to Drag Coefficients

Power and thrust requirements are shown for the chosen climb velocity at different angles while also comparing power and thrust requirements for different velocities with chosen climb angle $\alpha = 2^\circ$.

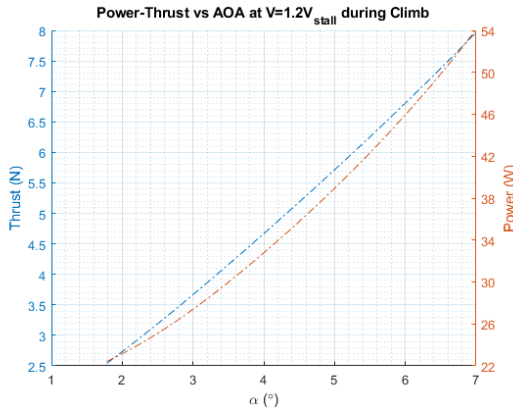


Figure 9: Power-Thrust vs AOA at $V = 1.2V_{stall}$ during Climb

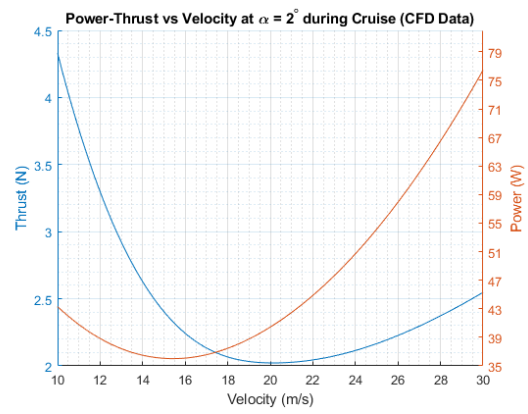


Figure 10: Power-Thrust vs Velocity at $\alpha = 2^\circ$ (CFD Data)

The motor chosen was *Leopard 2835-7T 1160 kV Brushless Airplane Motor* shown in figure 11 with a propeller size of 10 x 4.7 inches. Other options included the 5T, 6T and 8T versions which can be used together with other configurations. The motor has an efficiency of 75 % [15]. For a single three bladed propeller the *Leopard 2835-6T 1350 kV Brushless Airplane Motor* with a propeller size of 9 x 4.7 inches was chosen since the efficiency was higher with the 6T version for 9 inches and needs to run faster. For a dual two bladed propeller the *Leopard 2835-5T 1600 kV Brushless Airplane Motor* with a propeller size of 8 x 4.3 inches was chosen, for a three dual bladed propeller the same setup was used but with the rpm running 5 % lower.

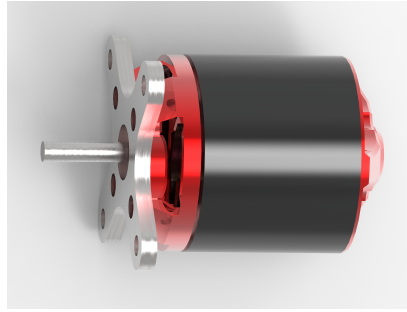


Figure 11: CAD of Motor (*Leopard 2835-7T*)

The propeller will be mounted on the back in a *Pusher* configuration.

Motor and Propeller Data:

Table 3: Motor and Propeller Data

Parameter	Meaning	Value	Unit
D_p	Propeller diameter	10	[in]
P_G	Propeller pitch	4.7	[in]
η_p	Propeller efficiency	0.64	[-]
η_{motor}	Motor efficiency	0.75	[-]
C_T	Thrust coefficient	0.0267	[-]
C_P	Power coefficient	0.0128	[-]
J	Advance ratio	0.3055	[-]
P	Max Motor power (without efficiency)	255.3	[W]
P_{AV}	Available motor power	122.5	[W]

3.3 Battery

Table 4: Battery data comparison of the *GA Soaring 2200 mAh 3S 20C Mini LiPo* and *Turnigy 5000mAh 3S 20C LiPo*

Model	GA soaring mini	Turnigy
Number	5	2
C-rating	20 C	20 C
Capacity	11 <i>Ah</i>	10 Ah
Max amps	44 <i>A</i>	100 A
Volt	11.1 <i>V</i>	11.1 V
Total weight	0.73 kg	0.69 kg
Cost	769 kr	650 kr
Specific energy	167 Wh/kg	160 Wh/kg
Energy density	400 Wh/L	331 Wh/L

Five batteries *GA Soaring 2200 mAh 3S 20C Mini LiPo* connected in parallel were chosen in order to balance the weight of the aircraft while also giving enough range and endurance to fly with more than 15 % extra range. It was also possible to choose bigger, heavier, and higher capacity batteries to gain an even greater range but since this is about optimisation of a mission profile these choices were made to cut down on cost and weight. The position of the batteries will be inside the fuselage according to figure 12. The batteries will be run in parallel to maximize capacity.

Battery Data:

Table 5: Calculated Data for battery

Parameter	Meaning	Value	Unit
C	Battery capacity	11000	[mAh]
C_{used}	Battery capacity used during flight	8000	[mAh]
U	Battery voltage	11.1	[V]
C_{rating}	C-rating	20	[C]
η_{batt}	Battery efficiency	0.95	[-]
m	Battery mass	0.73	[kg]
—	Dimensions	73x33x25	[mm]

3.4 Three-segment mission

Some general parameters such as total flight distance and stall speed are listed in table 6.

Table 6: General parameters

Parameter	Meaning	Value	Unit
R_e	Reynolds number	$7.6 \cdot 10^5$	[-]
V_{stall}	Stall speed	14.2	[m/s]
S_{total}	Total flight distance	111750	[m]
t_{total}	Total flight duration	3793	[s]
R	Total Range	162730	[m]
E	Total Endurance	5479	[s]
h	Height from takeoff to cruise altitude	100	[m]
$\mu_{asphalt}$	Friction coefficient for dry asphalt (without braking)	0.05	[-]
μ_{grass}	Friction coefficient for grass while sliding	0.16	[-]
$\mu_{launcher}$	Friction coefficient for launcher	0.05	[-]

During takeoff the motor will be running at a high speed (95 - 100 %) of maximum power ($\approx 12200 - 12900$ rpm) to make takeoff easier and faster to then begin the climb.

Takeoff parameters:

Table 7: Takeoff parameters

Parameter	Meaning	Value	Unit
$V_{takeoff}$	Takeoff speed	15.6	[m/s]
$S_{takeoff}$	Takeoff distance	54	[m]
$t_{takeoff}$	Takeoff time	6.9	[s]
$\alpha_{takeoff}$	Takeoff angle	0	[°]
$\Delta\alpha$	Change in AOA due to ground effect ($h = 30$ cm)	0.25	[°]
L_L	Launcher length	3	[m]
V_L	Launcher speed	17	[m/s]
F_L	Force needed for launcher	89	[N]

During the climb the motor will be running at 90 - 95 % of maximum power ($\approx 11600 - 12200$ rpm) to have enough power.

Climb parameters:

Table 8: Climb parameters

Parameter	Meaning	Value	Unit
V_{climb}	Climb speed	17	[m/s]
$V_{V_{climb}}$	ROC	1.8	[m/s]
S_{climb}	Climb distance	951	[m]
t_{climb}	Climb time	56.3	[s]
α_{climb}	Climb angle	6	[°]
P_{climb}	Power required for climb	45.9	[W]
T_{climb}	Thrust required for climb	6.8	[N]

For the cruise the motor will be running at 80 % of maximum power (≈ 10000 rpm).

Cruise parameters:

Table 9: Cruise parameters

Parameter	Meaning	Value	Unit
V_{cruise}	Cruise speed	30	[m/s]
S_{cruise}	Cruise distance	108000	[m]
t_{cruise}	Cruise time	3600	[s]
α_{cruise}	Cruise angle	2	[°]
$V_{stallturn}$	Stall speed in a turn	14.3	[m/s]
r	Radius of turn ϕ	117.7	[m]
t_{ψ}	Turn time for 180° turn	12.3	[s]
ψ	Turn rate	0.25	[°/s]
P_{cruise}	Power required	76.4	[W]
T_{cruise}	Thrust required	2.5	[N]

During the descent the motor will be running at 15 % of maximum power (≈ 1900 rpm) and will be used as safety much less performance.

Descent parameters:

Table 10: Descent parameters

Parameter	Meaning	Value	Unit
$V_{descent}$	Descent speed	20.9	$[m/s]$
$V_{V_{descent}}$	ROD	1.1	$[m/s]$
$S_{descent}$	Descent distance	1904	$[m]$
$t_{descent}$	Descent time	91.1	$[s]$
$\alpha_{descent}$	Descent angle	2	$[^\circ]$
$P_{descent}$	Power required	≈ 6.9	$[W]$

The landing distance with landing gear will roughly take twice the distance compared to belly landing. During touchdown the motor will be turned off.

Landing parameters:

Table 11: Landing parameters

Parameter	Meaning	Value	Unit
S_{tires}	Landing distance (tires)	114.4	$[m]$
S_{grass}	Landing distance (grass)	48.9	$[m]$
t_{tires}	Landing time (tires)	7.3	$[s]$
t_{grass}	Landing time (grass)	3.1	$[s]$

3.5 Mechanical Design and Integration

The battery is recommended to be fastened using a glue with high melting point and Velcro with additional straps around them. In order to not affect the CG too much the placement batteries will be made to offset the added weight of the motor with the weight of batteries. The CG is located 411 mm from the rear of the plane and is stationary due to the constant weight of the batteries during flight. One of the batteries should be place just above the CG and the other batteries is mounted as far from the CG as possible in the y-and x-direction. The batteries will further be placed to balance each others weight with 2 on each side of the CG. To add to the mass moment of inertia to prevent spinning and add more control and to distribute the load over the lift. A BWB configuration is considered trimmed (at the nominal cruise condition) when the aerodynamic center of pressure is coincident with the center of gravity. [16] To keep the the CG the battery placement is advised to be according to figure 12. The weight of wiring was not considered.

The propeller will be attached to a mount on the tail wing of the aircraft that is aerodynamically shaped in order to minimize the disturbance of laminar airflow.

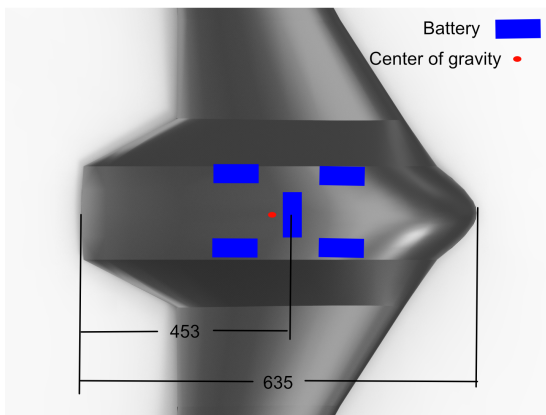


Figure 12: Battery Placement

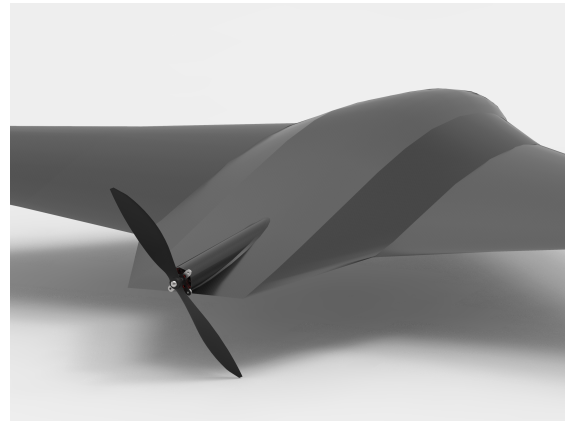


Figure 13: CAD Model of Mounting

4 Discussion

When choosing a propeller configuration, a large number of variables were considered and weighed, amongst them the placement, number, and size. The choice of using a *Pusher* configuration seemed the best because the airflow in front of the wing will not be affected and allows for more undisturbed air since measuring the flight characteristics is one the purposes with the prototype. One of the drawbacks, however is that the motor needs to be turned off during the takeoff if launched from a rail launcher. Having a dual-fan pusher setup was also considered, with the benefit of some redundancy and a greater possibility for flight control by controlling the propellers individually in turns. The major hurdle became the lack of space on the tail wing. Having a dual setup is, in general, more beneficial if space is available. The distance between the two propellers must be considered as disturbance may occur among them.

Most of the end choices for the final system configurations are based on benchmark data. When faced with the choice between benchmark test and data shown in the calculated variable, benchmark data were deemed more reliable and affected the choices to a higher degree. Furthermore, the benchmark data were obtained from one source, which gives it less reliability. Given that the calculated and approximated total efficiency is of essential for the accuracy of the whole project, a low efficiency estimation has been made to not under dimension the propulsion system. Most data were based on calculations and formulas from regular airplane configurations. The BWB is a fairly new concept, and not a lot of data is available. The ground effect on a BWB is, however taken into consideration with stall occurring earlier.

Going from conventional carbon-based fuel to hybrid fuel cells or even electrical does improve the environmental impact. However, performance is also of concern since batteries do not hold for long and take up a lot of space and weight on board the aircraft. Investing in solar panels for solar energy could be an interest as well. The size of the batteries could be made larger in the current system to improve range and endurance. If the battery is working at a high discharge rate at takeoff and landing the Peukert's law will have to be taken into consideration as the usable capacity will be lower.

The batteries have a safety margin partly because of safety and battery degradation. One battery could be taken out and it would still be able to fly for one hour with a safety margin. But due to the unknown battery efficiency and battery degradation one extra was added. Adding more batteries would add extra endurance and range up to the limit of 7 kg. The batteries were placed to maximize the mass moment of inertia to give more stability as the BWB is a light aircraft and can be affected by the wind. If a more agile plane desired, the batteries could be packed closer together. This will not have a massive effect at this scale but is something to consider for a larger model. The potential high temperature of the batteries is of concern. High temperatures are not just of concern for battery degradation, it is bad for the battery in several ways. Given the relatively high output of the batteries, long duration and styrofoam low thermal conductivity [17]. A

heat managing solution is advised, for example, an air intake. In case an air intake is to be made a careful consideration of the extra drag has to be made.

The optimal rate of climb has been calculated as information and guidance for the pilot and in case some autonomy is added to the aircraft with a possibility to opt for a lower climb angle for lower motor load. The rpm is kept at around 80 % to not push the motor to hard. Only going above for a short period of time during climb. The rpm were also kept between 100000 - 130000 to have low sound pollution and noise. The reasons a powered descent is chosen is because of control and stability. An unpowered decent where with only glide is however preferred for prolonging the battery, motor life and from an environmental perspective.

In order to minimize noise and maximize efficiency a single bigger propeller seems more reasonable with a lower rpm than 2 since they will need to run at a higher rpm since a dual propeller will need more rpm to generate the same amount of thrust needed. In case a single propeller fails with this aircraft it still has a high glide range when unpowered albeit with lower stability. It has its dangers as one motor failing will cause the aircraft to tilt and fly asymmetrical, in case of a *Tractor-Pusher* configurations. It would be plausible, but the front propeller would disturb the air coming towards the wing.

5 Conclusion

The final design of the power system resulted in an electric driven system with a single motor and a pusher propeller configuration. The Endurance objectives of at least 1 hour were reached with the resulting Endurance being 11 Ah. The maximum power used during the flight was 76 watts and well below the maximum available. The plane is powered by 5 Li-Po batteries with a total capacity of 11 Ah and a weight of 0.75 kg accompanied by a electric motor. This gives the aircraft a calculated total weight of 4 kg. Furthermore, the placement of the batteries was given a position that kept the CG in its original position while adding to the mass moment of inertia.

The 10 x 4.7 propeller was a good fit since rpm could be held at 10000 rpm for cruise which will keep noise to a minimum. Having a higher blade count did not seem necessary since the efficiency would drop down even more and is relatively low at 64 %. Since the amount of usable thrust is only 7 N which means with this motor the configuration is sufficient since the highest load is, according to given data, 6.8 N. The climb AOA was optimized since at maximum motor power, the chosen angle gives maximum ROC but lower AOA can be used to reduce motor load. The placement of the propeller was deemed the premier option since having them in front of the aircraft would ruin the whole concept of the project, which was to evaluate the blended wing, and placement in front of the wing disturbs the clean air on top of the airfoil.

6 Future Work

For future projects, it would be advised to go more in-depth on studying propeller types and if more propellers/blades could be beneficial depending on the placement/configuration. Had this been a bigger aircraft with a higher speed then a higher blade count could be an option because of the increased velocity and thrust needed. A variable-pitch propeller should be compared to fixed pitch to increase efficiency. Also optimizing the motor by having a more extensive motor study to get maximum efficiency is also something to be further researched. A wider range of motors could be examined. Ideally, a benchmark test with the chosen motor should be made.

Using different batteries could be better for the environment. Using a potential stabilizer on the wingtips could deem valuable or a small electric wing tip motor. This should be discussed for future projects like the full-scale Project "Green Raven" model.

References

- [1] N. Nacheva and G. Heldens, “The next generation of commercial supersonic flight: understanding the industry and the consumer perspectives,” 2018.
- [2] M. Kozek and A. Schirrer, *Modeling and control for a blended wing body aircraft: A Case Study*, 1st ed. Springer, 2015.
- [3] A. Barzkar and M. Ghassemi, “Electric power systems in more and all electric aircraft: A review,” *IEEE Access*, vol. 8, pp. 169 314–169 332, 2020.
- [4] E. Rivard, M. Trudeau, and K. Zaghib, “Hydrogen storage for mobility: a review,” *Materials*, vol. 12, no. 12, p. 1973, 2019.
- [5] B. Larrimer, *Beyond Tube-and-wing: The X-48 Blended Wing-body and NASA’s Quest to Reshape Future Transport Aircraft*, ser. NASA aeronautics book series. NASA, 2020. [Online]. Available: <https://books.google.com.mx/books?id=04dJzQEACAAJ>
- [6] R. Austin, *Unmanned aircraft systems: UAVS design, development and deployment*. John Wiley & Sons, 2011.
- [7] S. Gudmundsson, *General aviation aircraft design: Applied Methods and Procedures*, 2nd ed. Butterworth-Heinemann, 2021.
- [8] M. Sadraey, “Unmanned aircraft design: A review of fundamentals,” *Synthesis Lectures on Mechanical Engineering*, vol. 1, no. 2, pp. i–193, 2017.
- [9] F. Goetten, M. Havermann, C. Braun, F. Gómez, and C. Bil, *On the Applicability of Empirical Drag Estimation Methods for Unmanned Air Vehicle Design*. [Online]. Available: <https://arc.aiaa.org/doi/abs/10.2514/6.2018-3192>
- [10] F. Götten, D. Finger, M. Havermann, C. Braun, F. Gomez, and C. Bil, *On the flight performance impact of landing gear drag reduction methods for unmanned air vehicles*. Deutsche Gesellschaft für Luft-und Raumfahrt-Lilienthal-Oberth eV, 2018.
- [11] P. J. Swatton, *Principles of flight for pilots*. John Wiley & Sons, 2011.
- [12] Z. M. Salameh and B. G. Kim, “Advanced lithium polymer batteries,” in *2009 IEEE Power Energy Society General Meeting*, 2009, pp. 1–5.
- [13] J. S. Edge, S. O’Kane, R. Prosser, N. D. Kirkaldy, A. N. Patel, A. Hales, A. Ghosh, W. Ai, J. Chen, J. Yang *et al.*, “Lithium ion battery degradation: what you need to know,” *Physical Chemistry Chemical Physics*, vol. 23, no. 14, pp. 8200–8221, 2021.
- [14] M. Safari and C. Delacourt, “Aging of a commercial graphite/LiFePO₄ cell,” *Journal of The Electrochemical Society*, vol. 158, no. 10, p. A1123, 2011. [Online]. Available: <https://doi.org/10.1149/1.3614529>

- [15] FlyBrushless. (2022) Leopard - lc2835-8t. [Online]. Available: <https://www.flybrushless.com/motor/view/635>
- [16] R. H. Liebeck, “Design of the blended wing body subsonic transport,” *Journal of aircraft*, vol. 41, no. 1, pp. 10–25, 2004.
- [17] H. D. Young, *University physics*, 7th ed. Addison-Wesley Reading, MA, 1992.
- [18] A. Hobbies. (2022) Leopard lc2835 benchmark. [Online]. Available: https://cdn.shopify.com/s/files/1/0076/7098/8859/files/2835_new_chart.pdf?159&fbclid=IwAR3odeqLT8seTjPTpeaZ35BFIX3BR8pe4_2iZ1AzHmKXtytsD083d25HVr4



A Appendix

A.1 Aerodynamic Properties

Aerodynamic Values		Cd0	0,015	Aircraft Geometry		
α	CL	CD	Cdi	S	0,405	[m ²]
[deg]				c	0,36	[m]
-4,00	-0,054	0,0109	0,0002	b	1,25	[m]
-3,26	0,000	0,0110	0,0000	Atmospheric Properties		
-2,00	0,085	0,0111	0,0005			
0,00	0,223	0,0138	0,0032	ρ	1,225	[kg/m ³]
1,78	0,348	0,0184	0,0079	μ	1,74E-05	[Ns/m ²]
2,00	0,362	0,0190	0,0085			
4,00	0,501	0,0269	0,0163			
6,00	0,636	0,0377	0,0263			
6,50	0,669	0,0409	0,0291			
7,00	0,702	0,0444	0,0320			
7,50	0,734	0,0482	0,0350			
8,00	0,763	0,0524	0,0378			
8,50	0,789	0,0575	0,0404			
9,00	0,761	0,0739	0,0376			
9,50	0,760	0,0827	0,0375			
10,00	0,759	0,0925	0,0374			
12,00	0,665	0,1460	0,0287			
14,00	0,657	0,1900	0,0280			

Figure 14: Aerodynamic Properties

A.2 Benchmark of Motordata

LEOPARD HOBBY LC2835 Series Specification

Model	KV	No-load current	Max Amps	Propeller	Max Voltage	Current	Pull	Power	Efficiency	Load current	No. of Cells (Lipo)	Weight (motor only)**	Weight w/ hardware**	Shaft Diameter	Resistance	Length of Extended Shaft											
		(A)	(A)		(V)	(A)	(g)	(W)	(g/w)	(A)		(g)	(g)	(mm)	(ohm)	(mm)											
LC2835-4T	1880	1.5	39	0 7 5 0	7.4	14	400	103.6	3.9	33.5	2-3S	71	78	4	0.0315	12											
					8.4	17	550	142.8	3.86																		
					11.1	27	800	299.7	2.67																		
					12.6	36	1000	453.6	2.3																		
				0 8 4 3	7.4	20	870	148	5.88																		
					8.4	23	1060	193.2	5.49																		
					11.1	30	1400	333	4.2																		
LC2835-5T	1600	1.4	35	0 8 4 3	7.4	16	750	118.4	6.33	30	2-3S	71	78	4	0.0408	12											
					8.4	18	900	151.2	5.95																		
					11.1	23	1150	255.3	4.5																		
					12.6	26	1300	327.6	4																		
				0 9 4 7	7.4	22	1000	162.8	6.15																		
					8.4	24.5	1120	205.8	5.44																		
					11.1	32	1450	355.2	4.1																		
LC2835-6T	1350	1.2	32	0 9 4 7	7.4	15	800	111	7.2	27.5	2-3S	71	78	4	0.0468	12											
					8.4	17	950	142.8	6.65																		
					11.1	22	1250	244.2	5.12																		
					12.6	25	1400	315	4.45																		
					7.4	19	960	140.6	6.83																		
					8.4	22.5	1180	189	6.25																		
				1 0 4 7	11.1	29	1400	321.9	4.35																		
					7.4	25	1150	185	6.22																		
					8.4	29	1350	243.6	5.54																		
					8.4	17	980	142.8	6.86																		
					11.1	23	1400	255.3	5.48																		
					12.6	25	1580	315	5.01																		
LC2835-7T	1160	0.8	28	1 1 4 7	7.4	18	970	133.2	7.28	24	2-3S	71	78	4	0.0611	12											
					8.4	21.5	1170	180.6	6.48																		
					11.1	29.5	1600	327.45	4.89																		
				LC2835-8T	1038	0.7	24	1 0 4 7	7.4								10	650	74	11.5	21	2-3S	71	78	4	0.0818	12
									8.4								12	800	100.8	8							
									11.1								17	1190	188.7	6.3							
									8.4								15.5	980	130.2	7.53							
11.1	22	1400	244.2						5.73																		
12	25	1550	300						5.17																		
1 3 4 0	11.1	20.4	1300					226.44	5.74																		
	12.6	25	1620					315	5.14																		
	11.1	13.5	1010					149.8	6.74																		
	12	14.5	1135					174	6.52																		
	14	17	1360					238	5.71																		
	16.8	21	1600					352.8	4.54																		
LC2835-9T	900	0.6	20	1 1 4 7	8.4	12	830	100.8	8.23	17	2-4S	71	78	4	0.1023	12											
					11.1	17	1180	188.7	6.25																		
					14	22	1410	308	4.58																		
					7.4	9.5	600	70.3	8.5																		
					8.4	11	800	92.4	8.6																		
					11.1	16	1200	177.6	6.76																		
				1 3 4 0	12.6	18.5	1400	233.1	6																		
					14.8	23.8	1800	352.24	5.11																		
					7.4	6	440	44.4	9.9																		
					8.4	7	540	58.8	9.2																		
					11.1	10.5	900	116.55	7.7																		
					12	11.5	970	138	7																		
LC2835-10T	830	0.5	17	1 0 4 7	14.8	15.5	1340	229.4	5.8	14.5	2-4S	71	78	4	0.1332	12											
					12.6	15.5	1200	195.3	6.15																		
					14.8	18	1500	266.5	5.63																		
					16.8	22	1800	369.6	4.87																		
				1 3 4 0																							

Figure 15: Benchmark of Motordata [18]

A.3 CFD Data

1	4m span model		MAC (m)	0,964	e	0,88 W	245,25			
2	vinf (m/s)		S (m^2)	2,873	AR	5,569091542 k	0,06495059			
3	Re (based on MAC)	1,35E+06	rho (kg/m^3)	1,225		1,47E-05 cg (from nose)	0,718			
4	1	2	3	4	5	6	7	8	9	10
5	Cruise Velocity 5m/s		q		15,3125	V [m/s]		4,03E+05	447,0413615	
6	alpha (deg)	CL	CD	Cdi	PR0	PRi	PR	TR	L	L/D
7	-4,00	-0,0441	0,0137	0,0001	6,07	0,22	6,29	1,26	-1,94	-3,22
8	-3,36	0,0000	0,0138	0,0000	6,07	0,00	6,07	1,59	3,87	0,00
9	-2,00	0,0927	0,0140	0,0006	6,07	0,98	7,05	1,59	3,87	6,62
10	0,00	0,2290	0,0168	0,0034	6,07	5,99	12,06	4,93	9,94	13,63
11	2,00	0,3660	0,0223	0,0087	6,07	15,31	21,38	11,21	16,01	16,41
12	4,00	0,5010	0,0305	0,0163	6,07	28,69	34,76	20,43	22,08	16,43
13	6,00	0,6270	0,0423	0,0255	6,07	44,93	51,00	32,10	27,94	14,82
14	8,00	0,6480	0,0756	0,0273	6,07	47,99	54,06	33,69	28,64	8,57
15	10,00	0,5810	0,1170	0,0219	6,07	38,58	44,65	29,14	26,57	4,97
16		17,0727		18,9317	6,07	33314,37	33320,44	29,14	245,25	
17										
18										
19										
20										
21										
22	Cruise Velocity 20m/s		q		245	V [m/s]		20	1,61E+06	262,681245
23	alpha (deg)	CL	CD	Cdi	PR0	PRi	PR	TR	L	L/D
24	-4,00	-0,0516	0,0107	0,0002	151,6795997	2,43	154,11	7,71	-36,32	-4,82
25	-3,26	0,0000	0,0108	0,0000	151,6795997	0,00	151,68	7,58	0,00	0,00
26	-2,00	0,0870	0,0109	0,0005	151,6795997	6,92	158,60	7,93	61,24	7,98
27	0,00	0,2250	0,0136	0,0033	151,6795997	46,29	197,97	9,90	158,37	16,54
28	1,78	0,3484	0,0182	0,0079	151,6795997	111,00	262,68	13,13	245,25	19,13
29	2,00	0,3640	0,0188	0,0086	151,6795997	121,15	272,83	13,64	256,21	19,36
30	4,00	0,5020	0,0268	0,0164	151,6795997	230,42	382,10	19,11	353,35	18,73
31	6,00	0,6360	0,0378	0,0263	151,6795997	369,85	521,53	26,08	447,67	16,83
32	8,00	0,6540	0,0673	0,0278	151,6795997	391,08	542,76	27,14	460,34	9,72
33	10,00	0,6050	0,1080	0,0238	151,6795997	334,68	486,36	24,32	425,85	5,60
34	12,00	0,5710	0,1510	0,0212	151,6795997	298,12	449,80	22,49	401,92	3,78
35	14,00	0,5700	0,1900	0,0211	151,6795997	297,07	448,75	22,44	401,21	3,00
36	16,00	0,5900	0,2200	0,0226	151,6795997	318,29	469,97	23,50	415,29	2,68
37										

Figure 16: CFD Data

[illegible]

Figure 17: CFD Data

[illegible]

Figure 18: CFD Data

